Electrostatic resonances of heterostructures with negative permittivity: Homogenization formalisms versus finite-element modeling

Cédric Fourn and Christian Brosseau*

Laboratoire d'Electronique et Systèmes de Télécommunications (Unité Mixte de Recherche CNRS 6165), Université de Bretagne Occidentale, CS 93837, 6 avenue Le Gorgeu, 29238 Brest Cedex 3, France

(Received 24 July 2007; published 18 January 2008)

We investigate the effective permittivity ε of two-phase two-dimensional heterostructures, consisting of an inclusion (or cross section of infinite parallel, infinitely long, identical, cylinders, where the properties and characteristics are invariant along the perpendicular cross sectional plane), of permittivity $\varepsilon_2=\varepsilon_2'+\varepsilon_2''i$ with ε_2' being positive or negative, in a matrix of permittivity ε_1 (hereafter, assumed to be real valued and positive). Our method for computing $\varepsilon=\varepsilon'+\varepsilon''i$ is based on formulating the conservation of electric displacement flux through the interface separating the two media on systems with periodic boundary conditions in one direction. We identify two distinct behaviors in the surface fraction ϕ_2 dependence of the effective permittivity according the value of $\frac{|\varepsilon_2'|}{\varepsilon_1}$ relative to 1, which is a consequence of the duality symmetry. The incorporation of negative values of ε_2' into our calculations leads to a peak in $\varepsilon''(\phi_2)$ whereas $\varepsilon'(\phi_2)$ decreases to zero, which are both results of an electrostatic resonance (ER) phenomenon. We demonstrate that one can generate heterostructures characterized by an upward shift in the ER position as ε_2'' is increased. This suggests that, in principle, this property can be used to provide a wide range of innovative structures from specially designed composite materials, e.g., reconfigurable composite device. The comparison of our data with Maxwell Garnett (MG) and Bruggeman (SBG) homogenization formalisms permits a quantitative assessment of the ability of the two methods to capture the effects of surface fraction on ε. These methods have severe inadequacies, which arise physically from an incorrect treatment of the higher multipoles than dipole moments. We argue that the inappropriateness of SBG formula can originate from its prerogative that phase 1 and phase 2 are treated symmetrically. Our calculations show that MG formula may provide reasonable estimates for ε, even close to the ER position, of homogenized two-phase heterostructures with the real part of the complex-valued permittivities of phases having opposite signs and provided that $|\varepsilon_2'|\leqslant\varepsilon_2''$.

DOI: 10.1103/PhysRevE.77.016603 PACS number(s): 41.20.Cv, 02.70.Dh, 77.22.Ch, 77.84.Lf

While composite materials (CM) present a rich set of physical phenomena, many aspects of them are still poorly understood. The resolution of this problem has fascinated and confounded many generations of scholars, both theoretically and in the laboratory. With the advent of modern scientific computing, numerical simulations are being used to probe the generic features of the effective (relative) complex permittivity $\varepsilon=\varepsilon'+\varepsilon''i$ as a function of various couplings and interactions between components in the structure and due the presence of a hierarchy of length scales in these systems [1–8]. A special place in this field is occupied by the control of dielectric properties by exploiting the specific features of the electrostatic resonances (ER) [8–12]. From a theoretical point of view, ER occur when a metallic or dielectric particle (phase 2 of permittivity ε_2) with a negative real part of the permittivity is embedded in a dielectric host (phase 1 of permittivity ε_1) with a positive real part of the permittivity. Such ER, for which ε' decreases to zero while ε'' displays a peak, can occur only for special values of $\frac{\varepsilon_2}{\varepsilon_1}$ which have to be real and negative, e.g., for metal-in-insulator CM there is a range of frequencies between τ^{-1} (τ is the conductivity mean free time) and ω_p (the plasma frequency of the metal), where $\frac{\varepsilon_2}{\varepsilon_1}$ is very nearly real and negative [8,13]. These ER occur at the poles of $\frac{\varepsilon}{\varepsilon_2}$ when expressed as a function of $\frac{\varepsilon_2}{\varepsilon_1}$. McPhedran and McKenzie [14] have pictures of some of the ER for a square array of circular cylinders. While a great deal of insight into the position of these resonances as a function of geometric parameters has been gained, it has become equally clear that the proper design of the dielectric environment can result in dramatic effects in ER features. In addition, previous numerical investigations revealed that in arrays of elliptical particles with a core-shell structure embedded in a surrounding host, there exist so-called intrinsic ER (in the long-wavelength limit) whose features can be tuned by properly selecting the core and shell material parameters, and also the polarization of an electric field [12]. Experiments have taken advantage of these tunable parameters to study metamaterials, i.e., subwavelength sized structures which are intended to exhibit novel electromagnetic properties such as negative index of refraction [12,14–17]. Prompted by the link between ER, homogenization theory, and computational electromagnetism a number of researchers have begun to study the dielectric properties of artificially engineered CM in technologies for such applications as microwave biosensors, nanophotonics, and heterogeneous catalysis.

In many instances the effective permittivity ε of CM can be scaled to collapse to a common set of master curves

*Also at the Département de Physique, Université de Bretagne Occidentale.

described by $\frac{\varepsilon}{\varepsilon_1}=f\left(\frac{\varepsilon_2}{\varepsilon_1},\phi_2,A\right)$, where ϕ_2 denotes the surface fraction of phase 2, and the depolarization factor A ($0\leqslant A\leqslant 1$) is a functional of inclusion shape and permittivity mismatch only [4]. By now, a broad choice of analytic expressions is available for the function f which may score very well if compared to experimental or numerical data [1–8]. For example, the Maxwell Garnett (MG) [1–8] form for f is given by

$$f\left(\frac{\varepsilon_2}{\varepsilon_1},\phi_2,A\right)=1+\frac{\phi_2\left(\frac{\varepsilon_2}{\varepsilon_1}-1\right)}{1+A(1-\phi_2)\left(\frac{\varepsilon_2}{\varepsilon_1}-1\right)}. \tag{1}$$

Note that the roles of host and inclusion in Eq. (1) are not reciprocal. This result can also be derived by standard Lorentz local field arguments. In other instances, the function f is more complex, e.g., for Böttcher equation (also termed symmetric Bruggeman, SBG) [1–8], it can be computed as

$$f\left(\frac{\varepsilon_2}{\varepsilon_1},\phi_2,A\right)=\frac{1-A\left(1+\frac{\varepsilon_2}{\varepsilon_1}\right)+\phi_2\left(\frac{\varepsilon_2}{\varepsilon_1}-1\right)\pm\sqrt{\left[1-A\left(1+\frac{\varepsilon_2}{\varepsilon_1}\right)+\phi_2\left(\frac{\varepsilon_2}{\varepsilon_1}-1\right)\right]^2+4A(1-A)\frac{\varepsilon_2}{\varepsilon_1}}}{2(1-A)}. \tag{2}$$

Note that the roles of host and inclusion media are reciprocal. In this way of thinking the procedure amounts to finding the roots of a second-order polynomial and the physical root of Eq. (2) is determined from requirements of positivity of ε (or of the imaginary part ε'' of ε corresponding to dissipation). For many decades, Eqs. (1) and (2) were not challenged; they serve everyone well. When more attention was paid to the foundations of analysis, many started wondering about the limitations of these equations. More specifically, the dipolar nature of MG and SBG approaches fundamentally limits the range of applicability of Eqs. (1) and (2) [3,6–8]. It is often stated that laboratory or numerical data can be approximated arbitrarily accurately with Eq. (1) or Eq. (2) only in the dilute limit, i.e., when ϕ_2 is sufficiently small. However, delineating the precise limits of applicability of homogenization formalisms remains one of the major challenges for modern composite physics.

CM with interesting properties may be conceptualized if the real part of the complex-valued permittivities of the two-phase media have opposite signs. This situation is typical of metal-in-insulator CM for example, but our analysis is also relevant to the study of the previously mentioned metamaterials. This possibility has recently become feasible with the fabrication of dielectric-magnetic structures displaying a negative index of refraction in the microwave range of frequency [15,17]. The relative merits of the different homogenization approaches have been debated [2,5–8], but there have been relatively few comparisons of the different methods in the relevant CM. Quantifying the ER properties of this kind of CM versus composition can thus provide insights into polarization mechanisms of dielectric heterostructures and also improve our understanding of metamaterials and ultimately, the electromagnetic wave transport in unconventional CM.

In light of these theoretical results, the motivation for this work stems from a recent analytical study by Mackay and Lakhtakia (ML) [18] who have shown that homogenization formalisms have fundamental limitations when they are applied to deal with weakly dissipative component mediums characterized by permittivities with real parts of opposite signs. In this paper we take a step forwards remedying the abovementioned deficiency by presenting, for two-phase CM, a numerical study of how ε depends on $\frac{\varepsilon_2}{\varepsilon_1}$, the impact of inclusion shape on the ER positions, along with a comparison with analytics. Building on earlier work [4], the calculations discussed in this paper are carried out within a finite element (FE) based program which utilizes the conservation of electric displacement flux through an interface separating media. More importantly these results extend the ML analysis to CM containing specific inclusion shapes and with component mediums characterized by complex-valued permittivities whose real parts have opposite signs. A feature of our analysis is that we are able to quantify the degree to which different homogenization methods may capture the ER features.

Numerical calculations were performed using the FE Comsol MULTIPHYSICS software [19] and the procedure sorted out ε on a personal computer with a Pentium IV processor (3 GHz). By way of example, specific results are given below for a series of (nonoverlapping) inclusion with two simple shapes which are illustrated in Fig. 1(a). The CM discussed here are two-dimensional (2D) deterministic two-phase heterostructures [or cross sections of infinite parallel, infinitely long, identical, cylinders, where the properties and characteristics are invariant along the perpendicular cross sectional plane, with reference to Fig. 1(b)], where there is no source charge. In all cases, the simulation cell Ω is a square of length $L=1$. Periodic boundary conditions are enforced in the x direction for these structures. Comsol Multiphysics permits the closely controlled generation of FE meshes through the use of input files containing complete instructions for node-by-node and element-by-element mesh

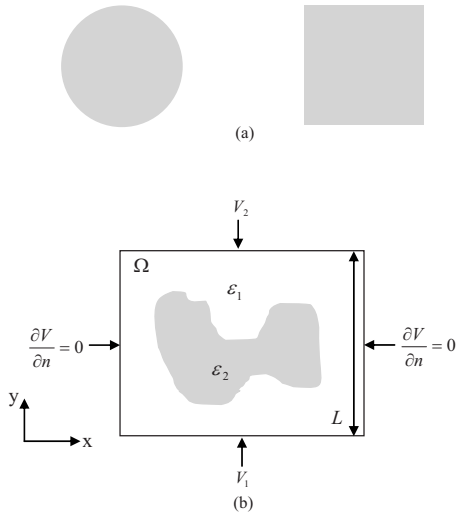

FIG. 1. (a) Schematic diagrams of the structural motifs of the inhomogeneous mixtures considered in this work. Two types of inclusions (gray region) are considered: disk and square. (b) Schematic illustration of the simulated cell employed to determine the effective complex permittivity of our model system consisting of a two-phase system, composed of a single 2D inclusion (phase 2 of permittivity ε_2), or cross section of an infinite cylinder, embedded in the host (phase 1 of permittivity ε_1). The model space can simulate a capacitor by applying a potential difference between the top and bottom faces of the model space. The evaluation of the effective permittivity, along the direction corresponding to the applied field, i.e., $\varepsilon=\varepsilon_y$, requires that the conservation of the electric displacement flux through the "surface" S has to be solved subject to appropriate the relevant boundary conditions for the potential. We fix $V_1=0$ V and $V_2=1$ V and assume that $\frac{\partial V}{\partial n}=0$ on the other side faces. L and S have both been set to unity.

specification, along with imposition of boundary conditions. In this work, the y axis was defined as pointing in the direction of the applied electric field. Omitting the details of derivation, which are similar to those described elsewhere [4], the effective (relative) permittivity along the direction corresponding to the applied field, i.e., $\varepsilon=\varepsilon_y$, can be found by integration via $\iint_S \varepsilon_i(x,y)\frac{\partial V}{\partial y}dxdy=\varepsilon(V_2-V_1)L$, where V_2-V_1 denotes the difference of potential imposed in the y direction, L is the size of the unit cell and S is the "surface" of the interface separating the two media. Since there is no induced polarization charge on the surfaces if the electric field is in the z direction, it is easy to show that $\varepsilon_z=\varepsilon_1+(\varepsilon_2-\varepsilon_1)\phi_2$. The potential on the top face of the square V_2 is fixed at a value of 1 V, while that on the bottom face V_1 is fixed at 0 V. For a disk, $A=\frac{1}{2}$ [4–6]. In the simulations $\phi_2 \leqslant \phi_{2c}$, where ϕ_{2c} corresponds to the touching inclusions limit in the regular lattice.

A technical remark is in order. While strictly correct only in a dc situation, these calculations can be extended to the quasistatic case for which, in general, $\varepsilon'' \neq 0$ and ε' may violate the dc restriction $\varepsilon' \geqslant 1$ [13]. In the case of electromagnetic radiation this means that all length scales must be much smaller than the wavelength of radiation and the skin depth (in case of a metal) or, equivalently, that the effective wave vector for the CM $k=\frac{\omega}{c}\sqrt{\varepsilon}\sqrt{\mu}=-\frac{\omega}{c}\sqrt{|\varepsilon|}\sqrt{|\mu|}$ should be much

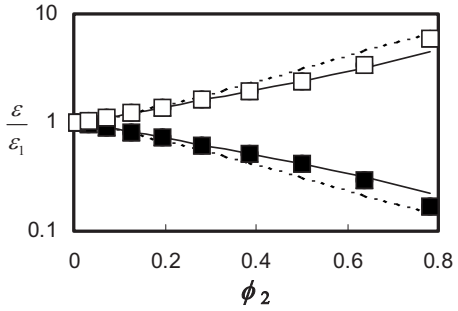

FIG. 2. Surface fraction of phase 2 dependence of the normalized effective permittivity of the 2D composite structure, composed of a circular inclusion in the matrix, to the matrix permitivity ε_1. The open circle, triangle, and square symbols correspond to ($\varepsilon_1=1$, $\varepsilon_2=10$), ($\varepsilon_1=10$, $\varepsilon_2=100$), and ($\varepsilon_1=100$, $\varepsilon_2=1000$), respectively. The solid circle, triangle, and square symbols correspond to ($\varepsilon_1=10$, $\varepsilon_2=1$), ($\varepsilon_1=100$, $\varepsilon_2=10$), and ($\varepsilon_1=1000$, $\varepsilon_2=100$), respectively. Observe that all symbols are superposed. Solid (dashed) lines show the values of ε as predicted by the MG (SBG) equation.

smaller than $\frac{1}{\xi}$, where ξ denotes a typical length scale that characterizes the inhomogeneities in the material medium, and c is the speed of light in vacuum.

As a preliminary test we have checked that our method reproduces known results for ideal nondissipative component mediums. Figure 2 illustrates the two-branch structure of the surface fraction dependence of the effective permittivity for a discoidal inclusion of component medium 2 embedded in the host component medium 1 [with reference to Fig. 1(a)]. The data presented are for different sets of ε_1 and ε_2. Examining all the data in Fig. 2, we first note that the upper branch (lower) corresponds to $\frac{\varepsilon_2}{\varepsilon_1}>1$ $\left(\frac{\varepsilon_2}{\varepsilon_1}<1\right)$. We assign the observed features in Fig. 2 to the Keller-Dykhne duality (or phase exchange) relation [6,7], i.e., $\varepsilon(\varepsilon_1,\varepsilon_2)\varepsilon(\varepsilon_2,\varepsilon_1)=\varepsilon_1\varepsilon_2$. In order to further understand the impact of $\frac{\varepsilon_2}{\varepsilon_1}$ on $\varepsilon(\phi_2)$ we have checked whether the MG and SBG estimates of ε (shown as curves in Fig. 2) can closely match the FE dielectric response. Comparison of the two theoretical curves and the FE data (all symbols are superposed) in Fig. 2 suggests that this can happen over a limited range of ϕ_2 values for SBG formula ($\phi_2<0.15$), but it is perhaps more surprising to observe that this can happen over a significant broader range for MG formula with discrepancies being significant close only if $\phi_2 \cong \phi_{2c}=\frac{\pi}{4}$. The standard argument to explain this behavior is that when the inclusions come close to each other the dipole approximation is no longer adequate since the nonuniformity of the field due to the other inclusions acting on a given inclusion becomes important. Higher multipoles than the dipoles must be used. Our results assume particular significance at large filling fractions because it is reasonable to hypothesize that we go beyond the lowest (dipolar) order to consider the effects of higher multipole interactions, which are absent in the MG and SBG approaches, which assume *a priori* that the polarization is electric dipole in nature, so higher-order electric terms are ignored. One of the formulas, SBG, is found to be significantly worse in the ability to capture the effect of ϕ_2 on ε. Further reflexion might suggest that the SBG formula fails for the fundamental rea-

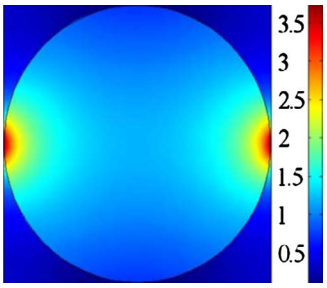

FIG. 3. (Color online) Local electric field enhancement factor $\frac{|\mathbf{E}(\mathbf{r})|}{E_0}$ for the 2D composite structure consisting of a circular inclusion in the matrix:$|\mathbf{E}(\mathbf{r})|$ (E_0) denotes the norm of the local electric field (the applied electric field). $\phi_2=0.782$. $\varepsilon_2=1$ and $\varepsilon_1=10$.

son that phase 1 and phase 2 are treated symmetrically. It is also instructive to see how the local-field varies in the spatial configuration that we considered. As further illustration we plot in Fig. 3 the local electric field enhancement factor $\frac{|\mathbf{E}(\mathbf{r})|}{E_0}$, where E_0 is the applied electric field. The observation of this plot goes against the notion of uniform electric field which underlies mean-field analysis and provides a hint for explaining the observed discrepancies between the numerical data and the predicted analytical values of ε [20,21].

We now focus on the case when the inclusion permittivity is a complex-valued quantity, e.g., $\varepsilon_2'=\varepsilon_1'$ and $\varepsilon_2''=1$. In Fig. 4(a), the calculated $\frac{\varepsilon'}{\varepsilon_1}$ is plotted against ϕ_2 along with the corresponding MG and SBG curves in order to explain the

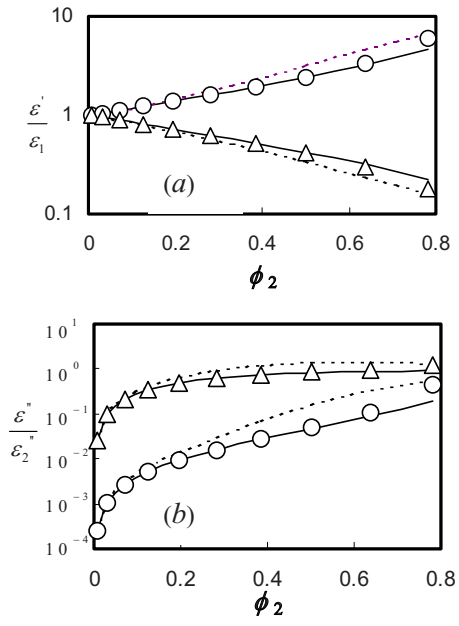

FIG. 4. (Color online) (a) The dependence of the real part $\frac{\varepsilon'}{\varepsilon_1}$ of the effective permittivity ε of a 2D composite structure consisting of a circular inclusion in the matrix as a function of the surface fraction of phase 2 and two values of $\frac{\varepsilon_2'}{\varepsilon_1'}$ and $\varepsilon_2''=1$. Symbols are (△) $\varepsilon_1'=10$ and $\varepsilon_2'=1$, (○) $\varepsilon_1'=1$ and $\varepsilon_2'=10$. Solid (dashed) lines show the values of ε as predicted by the MG (SBG) equation. (b) Same as in (a) for the imaginary part, $\frac{\varepsilon''}{\varepsilon_2''}$, of the effective permittivity.

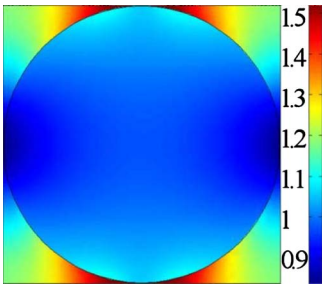

FIG. 5. (Color online) Local electric field enhancement factor $\frac{|\mathbf{E}(\mathbf{r})|}{E_0}$ for the 2D composite structure consisting of a circular inclusion in the matrix: $|\mathbf{E}(\mathbf{r})|$ (E_0) denotes the norm of the local electric field (the applied electric field). $\phi_2=0.782$. $\varepsilon_2=1+i$ and $\varepsilon_1=1$.

observed trends. Figure 4(b) gives the corresponding results for $\frac{\varepsilon''}{\varepsilon_2''}$. It is worth noting that the trend in Fig. 4(a) closely resembles that displayed in the previous nondisspative situation. We observed also (not shown) that the values of ε'' become more pronounced if ε_2'' is increased. Also shown, by the solid and dashed lines, are the expectation from the theoretical variation in ε' and ε'' with ϕ_2 from MG et SBG analysis, respectively. One can see that Eq. (1) models the data quite well even for the case of concentrated composite of dissipative inclusions. It is a particularly interesting result because irrespective of the details of the structure of the system, it can be shown [6,7] that Eq. (1) together with the complement formed by interchange of phases 1 and 2, form a pair of bound on ε. It should also be noted that the dashed line (SBG) reproduces the solid line (MG) for $\phi_2<0.15$. The color plot of Fig. 5 can yield quantitative information related to the the local electric field enhancement factor. From the plot it may be noted that the electric field inside the inclusion is not uniform.

Motivated by the above results, we proceed with a more in-depth analysis of the case of isotropic CM which arise from component mediums characterized by complex-valued permittivities whose real parts have opposite signs [22]. We consider an identical composite structure consisting of an isolated circular inclusion in the matrix and we assign the following sets of ε values corresponding to the different panels in Fig. 6. The upper panels, i.e., (a) and (b), show the evolution of ε as ϕ_2 is varied for $\varepsilon_1=10$ and $\varepsilon_2=-10+i$. The lower panels, i.e., (b) and (c), give the the corresponding values for $\varepsilon_1=1$ and $\varepsilon_2=-1+i$. The peak in ε'' is strongly reminiscent of the ER phenomenon. Based on the results of the FE simulations displayed in Fig. 6, a precise estimate of the ER position ϕ_{2r} can be obtained: ϕ_{2r} increases up to 0.05, and 0.447, in simulations performed at $\varepsilon_2=-10+i$, and $\varepsilon_2=-1+i$, respectively. With decreasing $|\varepsilon_2'|$, the ER is significantly broadened and attenuated. We have also compared the quantitative predictions of our simulations with SBG and MG models calculations. An obvious difference between the two curves is that SBG does not correctly predict the trends in ε' and ε'' over the accessible range of ϕ_2. It comes as a surprise that the MG reproduces quite well the ER profile, even when the ER position is outside the dilute limit, i.e., Figs. 6(c) and 6(d), and even if $|\varepsilon_2'|\gg\varepsilon_2''$, i.e., Figs. 6(a) and

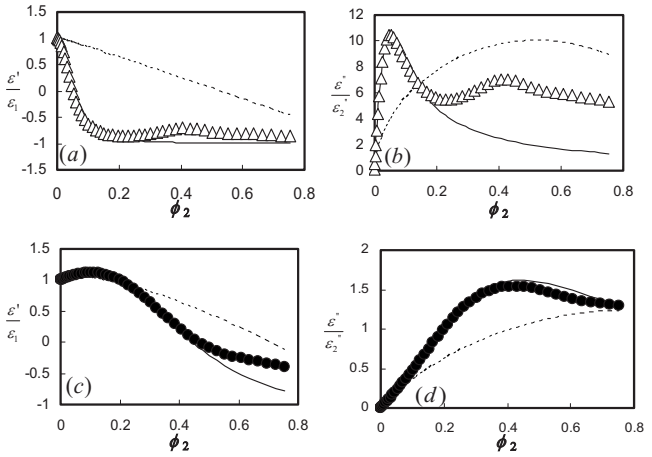

FIG. 6. (a) The dependence of the real part $\frac{\varepsilon'}{\varepsilon_1}$ of the effective permittivity of a composite structure consisting of a circular inclusion in the matrix as a function of the surface fraction of phase 2 and two values of $\frac{\varepsilon_2'}{\varepsilon_1'}$. $\varepsilon_2'=-\varepsilon_1'=-10$ and $\varepsilon_2''=1$. Solid (dashed) lines show the values of ε as predicted by the MG (SBG) equation. (b) Same as in (a) for the imaginary part, $\frac{\varepsilon''}{\varepsilon_2''}$, of the effective permittivity. (c) Same as in (a) for $\varepsilon_2'=-\varepsilon_1'=-1$ and $\varepsilon_2''=1$. (d) Same as in (b) for $\varepsilon_2'=-\varepsilon_1'=-1$ and $\varepsilon_2''=1$.

6(b). The fact that the SBG equation does not reproduce the correct ER position ϕ_{2r} for this kind of heterostructure is consistent with the recent analytical study of ML [18] who suggested that the SBG homogenization formalism is inapplicable for CM having two isotropic dielectric component mediums with $\varepsilon_1'\varepsilon_2'<0$ and $|\varepsilon_2'|\gg\varepsilon_2''$. Figure 7 allows us to visualize the electric field norm in the (x,y) plane corresponding to the resonant state of the upper panel of Fig. 6, which is significantly increased compared to what is observed in Fig. 5 ($\varepsilon_1'>0$ and $\varepsilon_2'>0$). The ER features were analyzed further with varying ε_2'' over two orders of magnitude. These results show that ϕ_{2r} upshifts as ε_2'' is increased (Fig. 8). For purpose of comparison, Fig. 8 also shows the evolution of ϕ_{2r} for three values of ε_2'. We would like to draw attention to the "S-shaped" profile observed for the different situations which is quite insensitive to the choice of ε_2' for the range of values of ε_2' considered.

Of particular interest here is the question of how shape anisotropy can influence the ER. The actual value of the

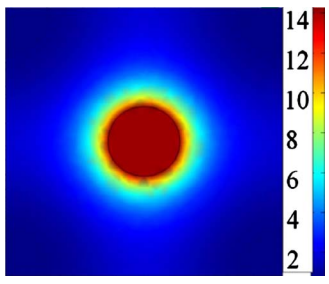

FIG. 7. (Color online) Local electric field enhancement factor $\frac{|\mathbf{E}(\mathbf{r})|}{E_0}$ for the 2D composite structure consisting of a circular inclusion in the matrix:$|\mathbf{E}(\mathbf{r})|$ (E_0) denotes the norm of the local electric field (the applied electric field). $\phi_2=0.053$. $\varepsilon_2=-10+i$ and $\varepsilon_1=10$.

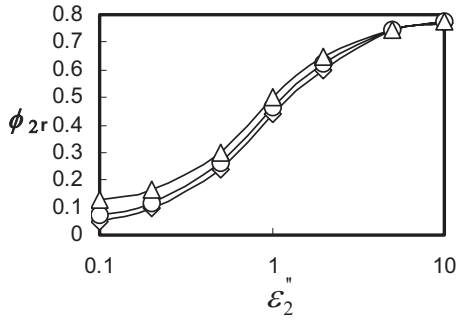

FIG. 8. Evolution of the surface fraction ϕ_{2r} corresponding to the ER of a composite structure consisting of a circular inclusion in the matrix as a function of ε_2''. Symbols are (♦) $\varepsilon_2'=-1$, (▲) $\varepsilon_2'=-0.8$, and (●) $\varepsilon_2'=-0.9$. The solid lines serve to guide the eye.

depolarization factor A for irregular inclusions of arbitrary shape is therefore of great practical importance. However, determining the value of this parameter is in general a challenging problem since not only does it depend on the particular geometry of inclusion but it can also depends on the permittivity ratio $\frac{\varepsilon_2}{\varepsilon_1}$, see, e.g., Ref. [4]. For that reason and to avoid demanding long-time simulations, we next examine the square inclusion sketched in Fig. 1(a) for which the accurate value of A are known [4], i.e., $A=0.43$. The values of ε are found in a fashion similar to the previously considered case of an isolated circular inclusion, under the same boundary conditions. Typical calculations of ε are shown in Figs. 9 and 10(a)–10(d) for the square inclusion without and dissipation, respectively. Under these circumstances, the dependence of $\frac{\varepsilon}{\varepsilon_1}$ versus ϕ_2 has a trend similar to the case of disk. The main point with Fig. 9 is its illustration of the duality symmetry which implies that $A\leftrightarrow 1-A$ when $\varepsilon_1\leftrightarrow\varepsilon_2$. Next we consider, in Fig. 10, the results for CM having component mediums characterized by complex-valued permittivities whose real parts have opposite signs. In addition, Fig. 10 compares the performance of Eqs. (1) and (2) to represent the behavior of $\frac{\varepsilon'}{\varepsilon_1}$ and $\frac{\varepsilon''}{\varepsilon_2''}$ with the FE data. In a similar fashion as was evidenced in the case of disk, decreasing $|\varepsilon_2'|$ significantly broadens and attenuates the ER profile. The comparison permits a quantitative assessment of the ability

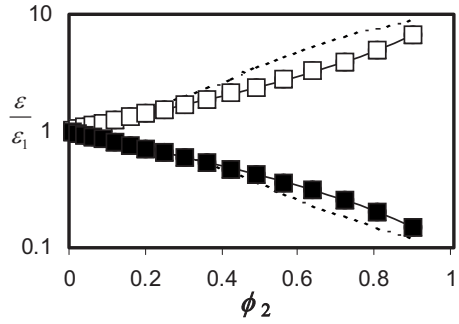

FIG. 9. Same as in Fig. 2 for a composite structure consisting of a square inclusion in the matrix. The computations were performed assuming $A=0.43$ in Eqs. (1) and (2) [4].

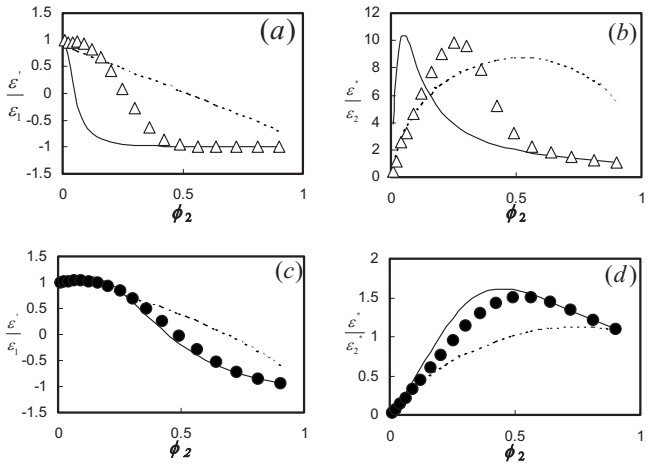

FIG. 10. Same as in Fig. 6 for a composite structure consisting of a square inclusion in the matrix.

of the two methods to capture the effects of ϕ_2 on ε and the ER profile. Several features of the results are important. First, for a dissipative inclusion medium with $|\varepsilon_2'| \gg \varepsilon_2''$, i.e., Figs. 10(a) and 10(b), none of the formalisms give a good treatment of $\varepsilon(\phi_2)$. Second, for a dissipative inclusion medium with $|\varepsilon_2'| \leqslant \varepsilon_2''$, it should be noted that the MG equation provides a better description of the data than the SBG, even close to the ER. In addition, the two curves superimpose in the dilute limit [panels (c) and (d)], which is consistent with the previous results of Figs. 6(c) and 6(d) corresponding to the discoidal inclusion. In Fig. 11, we display the ER position ϕ_{2r} for four values of ε_2'. The gradual shift of ϕ_{2r} with increasing ε_2'' is the salient feature, and is similar to that observed for the discoidal inclusion in Fig. 7. Results from numerical calculations of the local electric field enhancement factor are plotted in Fig. 12. The fourfold symmetry of the map is evident from this figure. The other noticeable feature of Fig. 12 is the nonuniformity of the electric field distribution in the square inclusion, especially around its boundaries, at the resonance.

We conclude with a few further comments. We start by observing that the above results are valid for the two simple shapes of inclusion considered. Other results can be expected for other inclusion geometries. For instance, one could con-

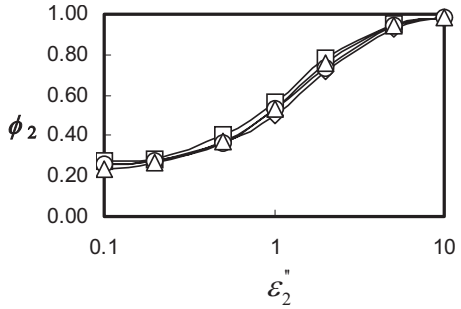

FIG. 11. Evolution of the surface fraction ϕ_{2r} corresponding to the ER of a composite structure consisting of a square inclusion in the matrix as a function of ε_2''. Symbols are (♦) $\varepsilon_2'=-1$, (■) $\varepsilon_2'=-0.7$, (▲) $\varepsilon_2'=-0.8$, and (●) $\varepsilon_2'=-0.9$.

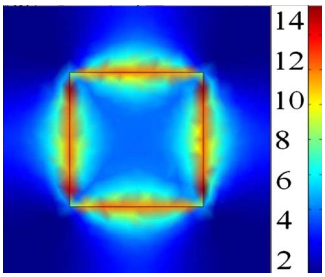

FIG. 12. (Color online) Local electric field enhancement factor $\frac{|\mathbf{E}(\mathbf{r})|}{E_0}$ for the resonant state of the 2D composite structure consisting of a square inclusion in the matrix. E_0 denotes the applied electric field. $\phi_2=0.25$, $\varepsilon_2=10+i$, and $\varepsilon_1=10$.

sider fractal inclusions, which have been studied in great detail in Ref. [4]. To illustrate the potential of our approach, we performed simulations to illustrate how the ER features are related to the shape of the inclusions and permittivity ratio between the inclusion and the matrix. Indeed, this suggests that, in principle, this property can be used to provide a wide range of innovative structures from specially designed composite materials, e.g., reconfigurable composite device with materials whose permittivity and magnetic permeability values may be designed to vary independently and arbitrarily throughout a material, taking positive or negative values as desired. Our study of the spatial distribution of the electric field gives information about the symmetry properties of the physical system in question. It should also be noted that the present results are not inconsistent with the interpretation of previous analytical calculations reported by ML in Ref. [18].

We now reexamine some of the notable trends in $\varepsilon(\phi_2)$ across the entire set of calculations. More importantly, our data reveal that neither of the two homogenization methods considered in this work give a particularly good treatment of the $\varepsilon(\phi_2)$ variation. These methods have severe inadequacies, which arise physically from an incorrect treatment of the higher multipoles than dipole moments. As such, the development presented here provides a method for the evaluation of the effective complex permittivity beyond the conventional dipolar MG approximation. The importance of the higher than two order multipolar interactions was recently stressed by Raab and co-workers [23]. In spite of evident commonalities, there is a crucial difference between the two approaches to homogenization considered here. Intriguingly, of the two analytical methods, MG is found to provide the better approximation to the FE estimation of ε, especially for dissipative inclusions even in the vicinity of the ER, albeit with the restriction that $|\varepsilon_2'| \leqslant \varepsilon_2''$, while the SBG formula cannot at least provide a qualitative prediction of the location of the ER. The reasons for this difference are as follows. First of all, the SBG formula derives from an effective medium approximation (EMA). The analysis is one of continuum physics: EMA approaches assume that each constituent is surrounded by the same effective medium. It assumes that the local electric field is the same in the surface occupied by each component in the composite. The analysis is done in the approximation of noninteracting inclusions (each inclusion is subject to the same mean field, unperturbed by the

presence of other inclusions). The accuracy and range of validity of EMA is not easy to establish. In principle, this approximation is rigorous at small surface fraction of inclusions (provided that their mutual positions are uncorrelated so that cluster-type configurations are excluded). In other words, in the effective medium the energy density is homogeneous by construction. It is also worth noting that what the matrix is and what an inclusion is are determined by the physical situation of the specific problem at hand, and it cannot be arbitrarily interchanged just to obtain an agreement with some calculations.

Lacking detailed information on the morphological features and on the material interfaces is the main short-coming of homogenization approaches. In spite of its relevance to explain the dielectric response of CM quantitatively, the role of microstructure has been largely neglected in simulation work to date. However, in special cases such as those presented here, the symmetry and duality of the theory are powerful enough to fix the exact (dipolar) couplings in the dilute limit. As mentioned earlier, these behaviors also have practical implications for the physics of metamaterials when the question of simultaneous negative permittivity and magnetic permeability is addressed [24,25].

Two comments, addressing possible extensions of the issue at hand, are in order. We would like to note that the long-wavelength limit for an arbitrary photonic crystal (PC) of 2D periodicity, i.e., periodic arrangement of infinite cylinders, was considered by many authors, e.g., Ref. [26]. PCs are artificial arrays of dielectric materials with 1D, 2D, or 3D periodicity. There is obvious similarity between the 2D periodic arrangement of infinitely long cylinders and the composites considered in the present work. Using the Fourier expansion method, the authors of Ref. [26] derived compact analytical formulas for ε of 2D PCs. In a previous work [2], we found that our numerical results are very close to those obtained by the Fourier expansion technique over the entire range of volume fraction [26,27]. In another perspective, considerable effort has been made to develop optical reflectance spectroscopy (RS) for analysis of heterostructures. Since the reflectance, i.e., the ratio of the energy of reflected to incident wave, is related to ε, e.g., Ref. [28], our numerical calculations can bring interesting information on the reflectance of composite structures containing inclusions with anisotropical dielectric properties, or irregular inclusions (geometrically complex interfaces and boundaries) for which analytical treatments are difficult to find. Since our analysis can be extended to treat electric fields that oscillate with time provided that the wavelengths and attenuation lengths associated with the fields are much larger than the microstructure dimension a detailed investigation of the effects of frequency in the reflectance at microwave to infrared frequencies of two-phase heterogeneous structures will be the subject of future work [29].

Lastly, we point out that the special cases considered here are limited by being only 2D and the range of inclusion geometries explored is unsufficient to carry out a complete numerical scheme to characterize the ER phenomenon of two-phase heterostructures. Our discussion of CM for which the real part of the complex-valued permittivities of the two phases have opposite signs does not exhaust the topic. Nevertheless, the present calculations show a rich variety of results and pave the way to understanding the linear dielectric response of more complex CM, i.e., with inclusions of irregular (nonsmooth) shape, anisotropy in permittivity, 3D, and arbitrary morphology, e.g., random, by showing that the two homogenization approaches previously considered are unsufficient to capture the main features of the composition dependence of the effective complex permittivity of heterostructures. We expect that the quantitative information about the limitation of two conventional approaches to homogenization reported in this paper will stimulate further theoretical work in this area.

We have benefited from discussions about technical points related to the material here with S. Lasquellec. The Laboratoire d'Electronique et Systèmes de Télécommunications is Unité Mixte de Recherche CNRS 6165.

[1] A concise treatment of the history of the theory of dielectric composites has been recently summarized in C. Brosseau, J. Phys. D **39**, 1277 (2006).
[2] C. Brosseau and A. Beroual, Prog. Mater. Sci. **48**, 373 (2003).
[3] V. Myroshnychenko and C. Brosseau, Phys. Rev. E **71**, 016701 (2005); V. Myroshnychenko and C. Brosseau, J. Appl. Phys. **97**, 044101 (2005).
[4] A. Mejdoubi and C. Brosseau, Phys. Rev. E **74**, 031405 (2006); A. Mejdoubi and C. Brosseau, J. Appl. Phys. **100**, 094103 (2006); A. Mejdoubi and C. Brosseau, *ibid.* **101**, 084109 (2007).
[5] A. H. Sihvola, *Electromagnetic Mixing Formulas and Applications* (IEE Publishing, London, 1999).
[6] S. Torquato, *Random Heterogeneous Materials: Microstructure and Macroscopic Properties* (Springer, New York, 2002).
[7] M. Sahimi, *Heterogeneous Materials I: Linear Transport and Optical Properties* (Springer, New York, 2003).
[8] D. J. Bergman and D. Stroud, in *Solid State Physics, Advances in Research and Applications*, edited by H. Ehrenreich and D. Turnbull (Academic, San Diego, 1992), Vol. 46, p. 147.
[9] G. Shvets and Y. A. Urzhumov, Phys. Rev. Lett. **93**, 243902 (2004).
[10] D. R. Fredkin and I. D. Mayergoyz, Phys. Rev. Lett. **91**, 253902 (2003). See also I. D. Mayergoyz, D. R. Fredkin, and Z. Zhang, Phys. Rev. B **72**, 155412 (2005).
[11] M. I. Stockman, S. V. Faleev, and D. J. Bergman, Phys. Rev. Lett. **87**, 167401 (2001).
[12] A. Mejdoubi and C. Brosseau, Phys. Rev. B **74**, 165424 (2006).
[13] See, e.g., L. Landau, E. M. Lifshitz, and L. P. Pitaevskii, *Electrodynamics of Continuous Media* (Butterworth-Heinemann, Oxford, 1984); J. D. Jackson, *Classical Electrodynamics*, 2nd ed. (Wiley, New York, 1975). The interested reader may also consult C. F. Bohren and D. R. Huffman, *Absorption and Scat-*

tering of Light by Small Particles (Wiley, New York, 1983).
[14] R. C. McPhedran and D. R. McKenzie, Appl. Phys. **23**, 223 (1980).
[15] See, e.g., R. A. Shelby, D. R. Smith, and S. Schultz, Science **292**, 77 (2001); D. R. Smith, J. B. Pendry, and M. C. K. Wiltshire, *ibid.* **305**, 788 (2004); J. B. Pendry and D. R. Smith, Phys. Today **57**, 37 (2004); D. R. Smith, W. J. Padilla, D. C. Vier, S. C. Nemat-Nasser, and S. Schultz, Phys. Rev. Lett. **84**, 4184 (2000); J. B. Pendry, A. J. Holden, W. J. Stewart, and I. Youngs, *ibid.* **76**, 4773 (1996).
[16] A. Alu and N. Engheta, IEEE Trans. Antennas Propag. **51**, 2558 (2003); N. Engheta, A. Salandrino, and A. Alu, Phys. Rev. Lett. **95**, 095504 (2005).
[17] A. V. Amirkhizi and S. Nemat-Nasser, J. Appl. Phys. **102**, 014901 (2007).
[18] T. G. Mackay and A. Lakhtakia, Opt. Commun. **234**, 35 (2004).
[19] Comsol MULTIPHYSICS Reference Manual, Comsol AB, Stockholm, Sweden, 2003.
[20] Y. Gu, K. W. Yu, and H. Sun, Phys. Rev. B **59**, 12847 (1999).
[21] D. Cule and S. Torquato, Phys. Rev. B **58**, R11829 (1998).
[22] It is important to note that no real CM can be found in resonant states characterized by special negative values of $\frac{\varepsilon_2}{\varepsilon_1}$ since no real material can have a permittivity ε that is real and negative—if $\varepsilon' < 0$, then there must be also a nonzero ε''. However, if ε'' is small, then the system can be excited to a state that is close to the ER. For example, the relative permittivity of silver is such that $\varepsilon' < 0$ but $\varepsilon'' \ll |\varepsilon'|$ at visible and near infrared wavelengths, see P. B. Johnson and R. W. Christy, Phys. Rev. B **6**, 4370 (1972); *Handbook of Optical Constants of Solids*, edited by E. D. Palik (Academic Press, New York, 1985). Thus, a CM made of silver inclusions are embedded in a dielectric host, e.g., silica, can exhibit ER if the wavelength of the externally applied electromagnetic field is in the visible or the near infrared range.
[23] A good entry point to the literature on multipole concepts is R. E. Raab and O. L. de Lange, *Multipole Theory in Electromagnetism* (Clarendon, Oxford, 2005); see also O. L. de Lange and R. E. Raab, Proc. R. Soc. London, Ser. A **459**, 1325 (2003); E. B. Graham, J. Pierrus, and R. E. Raab, J. Phys. B **25**, 4673 (1992).
[24] C. Caloz and T. Itoh, *Electromagnetic Metamaterials* (Wiley, New York, 2005).
[25] A. I. Căbuz, D. Felbacq, and D. Cassagne, Phys. Rev. Lett. **98**, 037403 (2007).
[26] P. Halevi, A. A. Krokhin, and J. Arriaga, Phys. Rev. Lett. **82**, 719 (1999); P. Halevi, A. A. Krokhin, and J. Arriaga, Appl. Phys. Lett. **75**, 2725 (1999); A. A. Krokhin, P. Halevi, and J. Arriaga, Phys. Rev. B **65**, 115208 (2002).
[27] R. Tao, Z. Chen, and P. Sheng, Phys. Rev. B **41**, 2417 (1990), see also C. Zhang, B. Yang, X. Wu, T. Lu, Y. Zheng, and W. Su, Physica B **293**, 16 (2000).
[28] A. Mejdoubi and C. Brosseau, Phys. Rev. E **73**, 031405 (2006); A. Mejdoubi and C. Brosseau, J. Appl. Phys. **99**, 063502 (2006).
[29] C. Fourn, S. Lasquellec, and C. Brosseau (unpublished).